Pharmaceutical Research, Vol. 9, No. 9, 1992

Research Article

Transport of Thyrotropin Releasing Hormone in Rabbit Buccal Mucosa *in Vitro*

Martin E. Dowty,[1,2] Kim E. Knuth,[1,3] Brian K. Irons,[1,3] and Joseph R. Robinson[1]

Received January 9, 1992; accepted March 3, 1992

The transport of thyrotropin releasing hormone (TRH) in rabbit buccal mucosa *in vitro* has been investigated with respect to (a) rate and type of metabolism of TRH on mucosal and serosal sides of buccal mucosa, (b) mechanism of TRH transport including charge effect on its permeability, and (c) pathway and rate-limiting regions of TRH movement. In addition, the integrity of excised buccal mucosa has been evaluated for purposes of *in vitro* solute diffusion experiments using tissue ATP level data, transmission electron microscopy, and TRH transport kinetic data. The results indicate that excised rabbit buccal mucosa can be used for TRH diffusion studies for approximately 6 hr. In addition, TRH apparently traverses buccal mucosa by simple diffusion with a steady-state permeability of about 10^{-7} cm/sec, and this permeability is independent of pH. Moreover, the primary pathway appears to be via the intercellular space in the rate-limiting barrier, i.e., the upper 50 μm of the epithelium. Finally, TRH is degraded predominantly by deamidase activity, which is followed by, to a lesser degree, carboxypeptidase metabolism.

KEY WORDS: thyrotropin releasing hormone; buccal mucosa; metabolism; permeability; *in vitro* tissue integrity; transport pathways; rate-limiting barrier.

INTRODUCTION

Recent advances in understanding of physiological functions of peptides and proteins and in efficient biotechnological production techniques have resulted in the need for their successful nonparenteral delivery (1–7). The preferred route, i.e., the gastrointestinal tract, is not an effective location to deliver peptides and proteins because of poor absorption, the presence of lumenal acids and enzymes, membrane related enzymes, and extensive first-pass hepatic metabolism. These types of limitations have led to the examination of various alternative delivery routes including buccal, sublingual, rectal, nasal, dermal, ocular, vaginal, and pulmonary mucosae.

Potential advantages of delivery through tissue in the mouth over other routes of administration include the following: (a) Sterile techniques are not required for drug administration; (b) gastrointestinal enzymes and acids and first-pass hepatic metabolism are avoided; (c) chronic or sustained therapy may be better tolerated relative to delivery via more fragile mucosa such as in the nose; (d) buccal mucosa is generally more permeable than the skin (8) but it has a limited usable surface area; (e) there is good accessibility for self-placement of a delivery system, for example, an adhesive patch, in a specific region and removal of the device in an emergency; and (f) one can modify permeability or inhibit proteases in a well-circumscribed area. However, tolerance limits of the tissue, especially with chronic drug delivery, need to be established. Zhang *et al.* (9) have recently shown that transbuccal insulin administration in dogs in the presence of the bile salt cholate shows an effect on blood glucose similar to that of an i.v. infusion of insulin. Moreover, the bile salt-treated tissue regained its permeability resistance 6 to 7 hr after removal of the enhancer.

The present study examines the buccal mucosa, i.e., the epithelium lining the cheek, as a potential site of peptide administration. The transport of thyrotropin releasing hormone (TRH) in rabbit buccal mucosa *in vitro* was evaluated with respect to (a) rate and type of metabolism of TRH on mucosal and serosal sides of buccal mucosa, (b) mechanism of TRH transport including charge effect on permeability, and (c) pathways and rate-limiting regions of TRH movement in buccal mucosa. Moreover, the integrity of excised buccal mucosa was evaluated for purposes of *in vitro* solute diffusion experiments. TRH is a tripeptide (L-pyroglutamyl-L-histidyl-L-proline amide) with a molecular weight of 362, an apparent pK_a of 6.2 (10), and an octanol/water partition coefficient of 0.0376 at pH 7.4 (11). TRH is metabolized rapidly in human plasma, with a half-life of about 5 min *in vivo* (12), making quantitation of this compound difficult in the systemic circulation. Consequently, *in vivo* TRH investigations usually monitor a secondary effect, in particular, thyrotropin and prolactin levels (13,14). In an effort to un-

[1] School of Pharmacy, University of Wisconsin-Madison, Madison, Wisconsin 53706.

[2] To whom correspondence should be addressed at Waisman Center, Room 607, 1500 Highland Avenue, Madison, Wisconsin 53705.

[3] Current address: Columbia Research Labs, 1202 Ann Street, Madison, Wisconsin 53713.

0724-8741/92/0900-1113$06.50/0

derstand TRH transport through buccal mucosa separate from other endogenous phenomena, the present study utilizes *in vitro* tissue mounted in a diffusion cell.

When performing solute diffusion studies, it is important to choose an appropriate animal model. Dogs, pigs, rabbits, and rhesus monkeys possess nonkeratinized mucosa which is ultrastructurally similar to the human cheek (15–19). Some of these species also share similar permeability characteristics (8,20–22). Thus, the rabbit buccal mucosa was selected for the present study.

MATERIALS AND METHODS

Materials

Unless otherwise stated, all chemicals, ACS reagent grade or better, were used as received and all solutions were prepared using distilled water which had been passed through a Barnstead PCS water purification system (DDW).

Tritiated TRH {[L-Pro-2,3,4,5-^{3}H(N)]-L-pGlu-L-His-L-ProNH$_2$ or ^{3}H-TRH; NEN Research Products, Du Pont, Wilmington, DE} with a specific activity of 119.2 Ci/mmol was used in diffusion cell studies. Radiochemical purity was determined by the manufacturer and our laboratory with thin-layer chromatography and HPLC (as described below) and purified, if necessary, to >99%. The tritium label on TRH was determined to be stable with rotovaporization techniques.

Removal of Rabbit Buccal Mucosa

Male albino New Zealand rabbits (Bakkom's Rabbitry, Viroqua, WI) were sacrificed with an overdose of 5% sodium pentobarbital injected into a marginal ear vein. The buccal mucosa was removed and remaining muscle and underlying submucosal tissue were subsequently stripped away using very fine-point forceps and Castro-Viejo scissors under a dissection scope (Nikon Model SMZ-1B). The tissue was rinsed/stored in ice-cold saline until mounted in the diffusion cell.

Diffusion Cells

Two side-by-side diffusion cells were used: (a) a large-volume diffusion cell (Jim's Instrument Manufacturing, Inc., Iowa City, IA; UW-Machine Shop, Madison, WI) of the type described by Schoenwald and Huang (23) and Veillard *et al.* (24), which was originally designed for corneal permeability studies and has been well characterized with respect to its hydrodynamic aspects (25); and (b) a small-volume diffusion cell and water-jacketed block heater of the type described by Grass and Sweetana (26) (Precision Instrument Design, Los Altos, CA).

In Vitro Tissue Integrity Assessment

ATP Levels. The amount of ATP (nmol/g tissue) was determined in rabbit buccal mucosa immediately after excision and at various times up to 6 hr under TRH permeability study conditions (see below). The method of ATP extraction using perchloric acid as the extractant and subsequent assay (bioluminescent assay, Sigma, St. Louis, MO) was followed as reported by Longer (20). The extraction efficiency was found to be greater than 90%.

Transmission Electron Microscopy (TEM). Rabbit buccal mucosa was fixed in 4% glutaraldehyde after being freshly excised and after incubation under TRH permeability study conditions (see below) for 3 to 6 hr. Further sample preparation was performed by the Centralized Electron Optics Facility (Anatomy Department, University of Wisconsin, Madison, WI) as follows: Tissue specimens were rinsed in 0.1M phosphate buffer, fixed in 2% buffered osmium tetroxide, rinsed again in phosphate buffer, dehydrated in alcohol, and embedded in Durcupan ACM (Fluka). Sections of 70 nm were cut, stained with uranyl acetate–lead citrate, and visualized with a Hitachi H-600 electron microscope.

Transport Kinetics. TRH diffusion experiments were performed up to 18 hr under TRH permeability study conditions (see below).

TRH Metabolism Studies

The following buffer was prepared and preequilibrated to 37°C: 25 m*M* HEPES, isotonic with 0.8% NaCl (298 mOsm) at pH 7.4. Osmolarity was measured on a Wescor 5500 vapor pressure osmometer (Logan, UT). The pH was adjusted with small amounts of concentrated NaOH or HCl.

Freshly prepared rabbit buccal mucosa was mounted in a large-volume diffusion cell (epithelial side facing the donor chamber) at 37°C. Subsequently, 15 μCi/ml (1.26×10^{-4} m*M*) ^{3}H-TRH in the above specified buffer was added to both the donor and the receiver chambers. The pH of the bathing buffers did not change by more than 0.2 pH unit during the course of the experiment. The donor and receiver bathing solutions were then sampled from 0 to 4 hr. Each sample was worked up with the following extraction procedure (27,28) prior to HPLC injection: (a) add 2 parts acetonitrile (HPLC grade) to 1 part sample; (b) vortex for 1 min and centrifuge at full speed for 15 min (Dynac Centrifuge, Cat. No. 0101, Becton Dickinson and Co., Parsippany, NJ); (c) remove an aliquot of the supernatent and dry under N_2 gas in a block heater set at approximately 37°C; (d) reconstitute the dried residue with 50 μl of DDW; and (e) inject 20 μL of this preparation onto the HPLC system described below. Using the above extraction procedure, the percentage recovery of TRH was between 95 and 100%, and moreover, the tripeptide was stable.

The HPLC system used in the analysis of TRH and its metabolites consisted of two columns: a LiChroCART, LiChrosorb 100 RP-18 precolumn and a Phenomenex, Zorbax ODS, 250 × 4.6-mm column. The mobile phase was made up of the following: 0–2% methanol (HPLC grade), 0.1% H_3PO_4, in DDW. The pH was adjusted to 7.0 with a small amount of concentrated NaOH. The mobile phase was filtered through a Millipore filtering system (Millipore, Bedford, MA) using Metricel membrane filters (0.45 μm; Gelman Sciences Inc., Ann Arbor, MI) and degassed under vacuum. The flow rate was set at 1 ml/min (Beckman 110B pump, Beckman Instruments Inc., Berkeley, CA) and the absorbance was adjusted to 220 nm (Perkin Elmer LC-75 spectrophotometric detector, Worwick, CT). Retention times for Pro, Pro-NH_2, pGlu-His-Pro, cyclo-His-Pro, and TRH were 2.8, 3.6, 6.6, 8.8, and 12 min, respectively, and

varied slightly with the amount of methanol in the mobile phase.

After injection of the sample, the HPLC eluant was collected in scintillation vials at 0.5-min intervals. Vials were then filled with 10 ml Bio-Safe II (Research Products International Corp., Mount Prospect, IL) and counted on a Tri-Carb 460CD (Packard Instruments, Downers Grove, IL) using the external standard channels ratio method of quench correction to determine counting efficiency.

TRH Permeability and Mechanism of Transport Studies

The following buffers were prepared: (a) *HEPES buffer*—10–50 m*M* HEPES and 30 mg/ml of nonradiolabeled TRH (Sigma), isotonic with NaCl at pH 8.0; and (b) *citric acid buffer*—10–60 m*M* citric acid and 30 mg/ml of nonradiolabeled TRH, isotonic with NaCl at pH 4.0. The bathing solutions contained 30 mg/ml (83.3 m*M*) of nonradiolabeled TRH in an attempt to saturate metabolic enzymes in the tissue (see Results and Discussion). From metabolism studies, maximal TRH metabolism on the serosal side of the tissue was calculated to be 2.7×10^{-5} *M* hr^{-1} cm^{-2}. Hence, the amount of nonradioactive TRH (i.e., 83.3 m*M*) is, for the most part, constant during the experiment in that more than 99.9% of the cold tripeptide remains in the receiver chamber after 1 hr, at which time the receiver solution is replaced with 83.3 m*M* fresh nonradioactive TRH.

Freshly excised buccal mucosa was preequilibrated with the buffer of interest for 30 min before the start of the diffusion experiment at 37°C. The tissue was then mounted in a small-volume diffusion cell with the mucosal side facing the donor compartment. Subsequently, approximately 15 μCi/ml (1.26×10^{-4} m*M*) to 50 μCi/ml (4.19×10^{-4} m*M*) of ^{3}H-TRH in either *HEPES buffer,* pH 8.0, or *citric acid buffer,* pH 4.0, was added to the donor side, while an equal volume of the same buffer without radiolabeled TRH was added to the receiver side. A sample of the donor chamber was taken to establish the initial concentration of TRH. The pH of the bathing buffers did not change by more than 0.2 pH unit during the course of the experiment. Since solute permeability across the two cheeks of the same rabbit is usually identical, one of the two cheeks was used with the pH 4 buffer, while the other was used with the pH 8 buffer in an effort to decrease interrabbit variability. Multiple samples were taken from 0 to 4 hr from both donor and receiver chambers for both direct radiometric analysis and HPLC workup (as described above).

TRH Pathway and Rate-Limiting Barrier Studies

Microautoradiography. Freshly excised rabbit buccal mucosa was incubated for 4 hr at 37°C in a large-volume diffusion cell, containing approximately 25 μCi/ml of ^{3}H-TRH in isotonic Krebs–Ringer bicarbonate (KRB) buffer, pH 7.4, in the donor compartment and the same buffer without TRH in the receiver compartment. The buccal tissue was placed in the diffusion cell with the mucosal side or serosal side facing the donor compartment in separate experiments. Control tissues were not exposed to ^{3}H-TRH.

At the end of 4 hr, tissue were fixed in 4% paraformaldehyde/0.1% glutaraldehyde, rinsed in phosphate-buffered saline, dehydrated in alcohol, and embedded in epon. Serial 2-μm sections were made on a Sorvall Porter-Blum Ultra Microtome MT-2 (Norwalk, CT). In a darkroom, sections were then dipped in Kodak Nuclear Track Emulsion (Type NTB2, Eastman Kodak Co., Rochester, NY), placed in a plastic micro slide box (VWR Scientific, Chicago, IL), and light-tight sealed with tape. The slides were exposed for 2 to 8 weeks in a 4°C refrigerator. Some slides were light fogged before being placed in boxes to check for negative chemography (2).

The slides were developed according to the following protocol: (a) 2.5 min in full-strength Kodak developer D-19, (b) a 1-min rinse in DDW, (c) 3 min in 1 part Kodak rapid fix:2 parts DDW, and (d) a 1-min rinse in DDW. After air-drying, sections were stained with 1% toluidine blue in 0.2 *M* phosphate buffer, pH 7.4, for 5 sec on a 70°C hot plate.

Osmolarity Experiments. The following buffers were prepared: (1) pH 4 *citric acid buffer*—30 m*M* citric acid and 30 mg/ml nonradioactive TRH including various amounts of mannitol to make 120, 320, and 495 mOsm solutions; and (2) pH 8 *HEPES buffer*—25 m*M* HEPES and 30 mg/ml nonradioactive TRH including various amounts of mannitol to make 120, 302, and 537 mOsm solutions.

Freshly excised buccal mucosa was preequilibrated with the buffer of interest for 30 min at 37°C before the start of the diffusion experiment. After mounting the tissue into a small-volume diffusion cell, 1 to 2 μCi/ml of ^{3}H-TRH in 1.2 ml of either HEPES or citric acid buffer, listed above, was added to the mucosal side of the tissue (i.e., donor compartment). An equal volume of the same buffer was placed in the receiver chamber without ^{3}H-TRH. The rest of the diffusion study was carried out as described above. Since the solute permeability across the cheeks of the same rabbit is usually identical, one of the two cheeks was always used under isotonic conditions, while the other was used under either hypotonic or hypertonic conditions to decrease interrabbit variability.

RESULTS AND DISCUSSION

In Vitro Tissue Integrity Assessment

Table I summarizes the calculated amounts of ATP in rabbit buccal mucosa with time. These results indicate that ATP drops approximately 30% after 3 hr and 40% after 6 hr.

Table I. ATP Levels in Rabbit Buccal Mucosa *in Vitro*

Time after excision (hr)	n^a	ATP (nmol/g tissue)
0	15	105 (4.6)[b]
1	17	73 (4.9)
2	15	71 (3.2)
3	10	67 (5.6)
4	9	64 (5.3)
5	10	63 (3.9)
6	9	60 (5.3)

[a] Number of determinations.

[b] Number in parentheses represents 90% confidence limits (two-tailed *t* distribution).

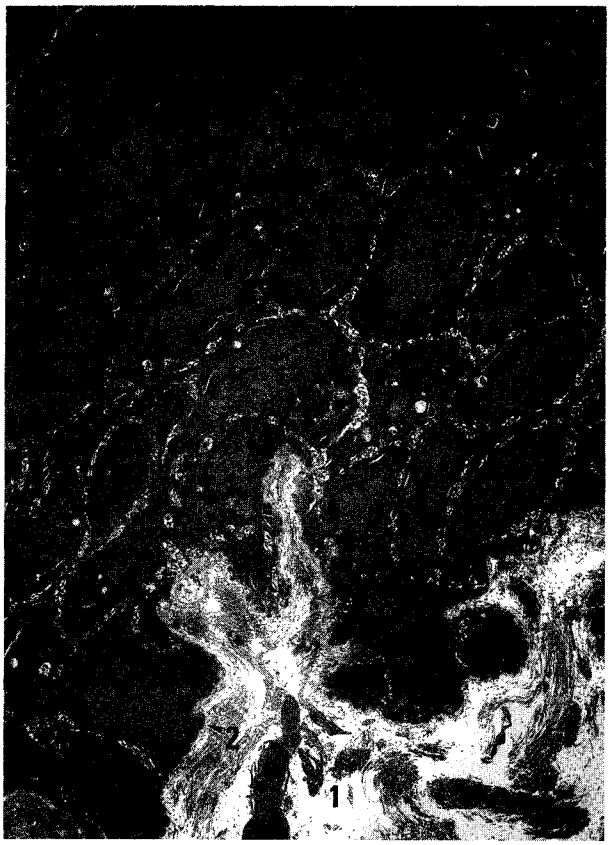

Fig. 1. Electron micrograph of the lower epithelial cells and connective tissue of rabbit buccal mucosa after 3 hr *in vitro* (representative of 0 hr *in vitro*). Note the location of connective tissue (1), basement membrane (2), basal cells (3), and prickle cells (4). 3800×; reduced to 70% for reproduction.

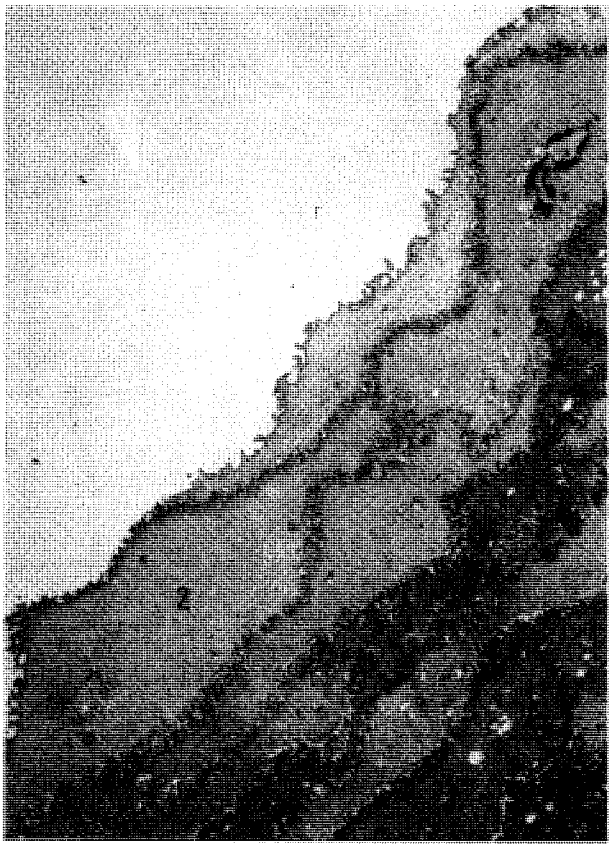

Fig. 2. Electron micrograph of the upper epithelial cells of rabbit buccal mucosa after 3 hr *in vitro* (representative of 0 hr *in vitro*). Note the location of intermediate cells (1) and superficial cells (2). 2900×; reduced to 70% for reproduction.

Figures 1 through 3 are TEM photos of excised tissue after 3 and 6 hr. Freshly excised mucosa could not be distinguished from 3-hr tissue and are not shown here. On the other hand, 6-hr tissue showed obvious signs of structural breakdown in the lower epithelial cell layers, i.e., cell–cell separation and vacuole formation, indicative of cell death (Fig. 3). However, intermediate and superficial cells at 6 hr are structurally similar to freshly excised and 3-hr tissue (Fig. 2). A representative plot of TRH transport data to 18 hr is shown in Fig. 4. After a short lag time, the slope of the line is relatively constant, i.e., steady state, between 2 and 8 hr, at which time, TRH permeability progressively increases, indicating that changes are occurring in the rate-limiting barrier.

By itself, ATP levels do not indicate the structural integrity of excised tissue but, rather, reveal the metabolic capacity of the tissue. However, it is not clear what level of cellular ATP is necessary for normal function of the tissue. Microscopy and transport data showed that, for at least 6 hr, the upper cell layers, i.e., rate-limiting step (see below), remain structurally intact and steady-state kinetics are seen. The more superficial cells begin to deteriorate at around 8 hr, coincident with increasing TRH permeability. To this end, it appears that excised rabbit buccal mucosa can be used for TRH diffusion studies for approximately 6 hr. For the purposes of the present study, all experiments were completed within 4 hr.

Metabolism of TRH

When TRH is applied to both mucosal and serosal sides of excised rabbit buccal mucosa, the rate and extent of metabolism are different as summarized in Table II. TRH is largely susceptible to TRH deamidase activity, yielding pGlu-His-Pro (TRH-OH). This pathway is followed by, on the serosal side only, Pro carboxypeptidase degradation of TRH-OH, resulting in the formation of pGlu-His and Pro. No pGlu aminopeptidase degradation of TRH was detected. It is possible that pGlu-His was degraded further to pGlu and His, but it would not be apparent with this method of analysis.

The rate constants of TRH disappearance for the donor and receiver solutions were determined to be 5.8×10^{-6} M hr^{-1} cm^{-2} (correlation coefficient, $R = 0.973$) and 2.7×10^{-5} M hr^{-1} cm^{-2} ($R = 0.993$), respectively. In effect, as TRH traverses buccal epithelium, metabolism appears to follow a biphasic pattern. The tripeptide will initially encounter some deamidase activity at the epithelial surface, while at

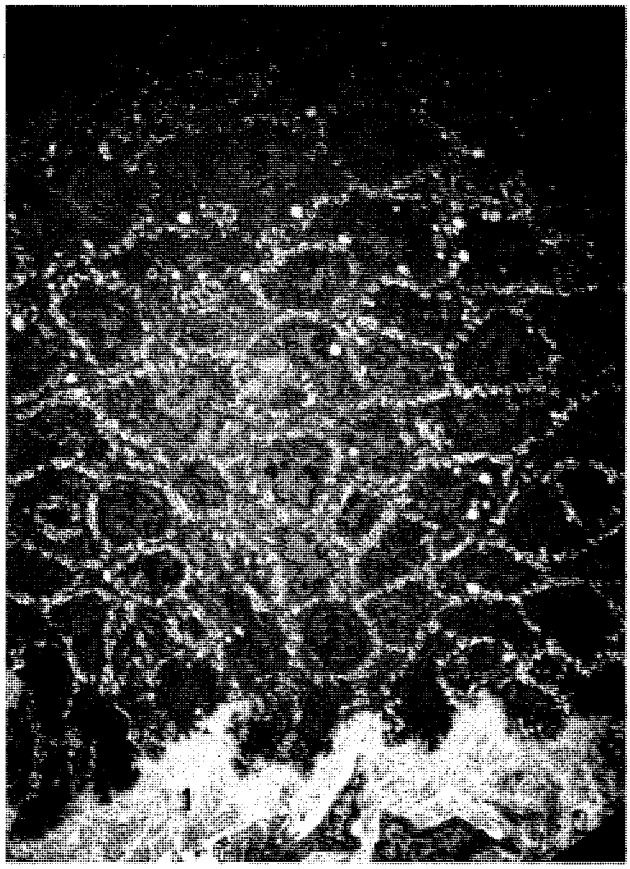

Fig. 3. Electron micrograph of the lower epithelial cells and connective tissue of rabbit buccal mucosa after 6 hr *in vitro*. Upper epithelial cells were similar to those seen at 0 and 3 hr *in vitro* (Fig. 2). The locations of the connective tissue (1), basal cells (2), and prickle cells (3) are indicated. Note the magnitude of cellular separation occurring, especially in the basal cell layers. 1900×; reduced to 70% for reproduction.

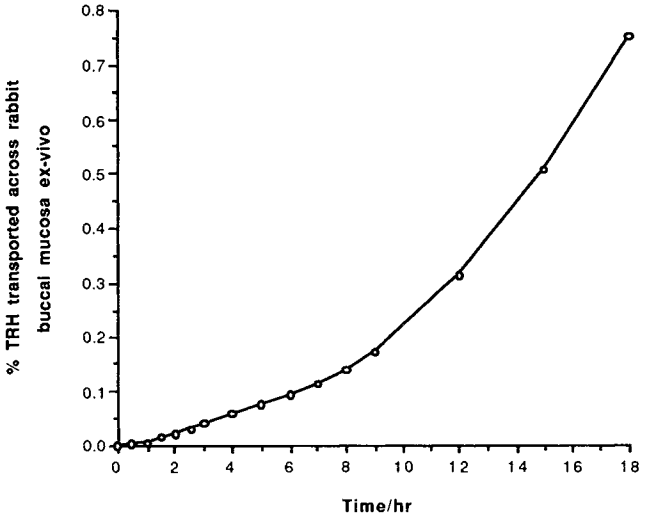

Fig. 4. Representative plot of TRH permeability in rabbit buccal mucosa *in vitro* from 0 to 18 hr. Note the linearity of the curve from 2 to 8 hr, where subsequently TRH permeability increases progressively.

some point in or below the rate-limiting barrier, deamidase metabolism increases and carboxypeptidase activity appears. The change in metabolism rates may be correlated to different pathways for TRH in and below the superficial permeability barrier (see below).

Peptidase activity in tissue homogenates from various sites of administration, such as nasal, buccal, intestinal, rectal, vaginal, and ocular mucosae, have been identified (28–31). Although these results represent an indication of maximal hydrolytic activity in the tissue, the enzymes may be localized at various sites in and around the cell, for example, in lysosomes, secretory vesicles, or the extracellular space. Hence, the peptide or protein may or may not be exposed to certain peptidases, depending on its pathway of movement through the mucosa. To this end, analysis of peptide or protein metabolism in intact mucosa *in vitro* should approximate, to a greater degree, the degradation of the compound as it crosses the tissue. Moreover, isolation of the tissue allows for distinction between metabolism occurring in the tissue vs the rest of the body.

While these results clarify TRH metabolism in rabbit buccal mucosa, the following issues remain unanswered: (a) gradual cellular changes in the excised mucosa during the diffusion study resulting in enzymes being released from cells (however, the rate of metabolism remained relatively constant over time in our studies); (b) residual enzymes released from cellular components in the connective tissue during buccal mucosa preparation to remove underlying muscle and submucosa; and (c) the fact that enzymatic TRH

Table II. Summary of TRH Metabolism (1.26×10^{-4} m*M*) in Rabbit Buccal Mucosa *in Vitro*[a]

Mucosal metabolism of TRH (donor chamber)		
	Percentage	
Time (hr)	TRH	TRH-OH
0	99 (±0)	1 (±0)
1	93 (±1)	6 (±1)
2	90 (±1)	9 (±1)
3	87 (±1)	13 (±1)
4	84 (±1)	16 (±1)

Serosal metabolism of TRH (receiver chamber)			
	Percentage		
Time/hr	TRH	TRH-OH	Pro
0	99 (±0)	1 (±0)	0 (±0)
1	82 (±3)	16 (±2)	2 (±1)
2	62 (±3)	35 (±2)	3 (±1)
3	45 (±3)	50 (±2)	5 (±1)
4	33 (±4)	59 (±3)	8 (±1)

[a] TRH, pGlu-His-ProNH_2; TRH-OH, pGlu-His-Pro; Values are averages of three experiments. Numbers in parentheses represent standard errors of the means.

degradation *in vitro* may have been overestimated in comparison to the *in vivo* situation, where solute is removed by the capillary circulation (32,33).

Permeability and Mechanism of Transport of TRH

An apparent permeability coefficient (P), or velocity of transport, can be calculated for TRH once the magnitude of metabolism of the solute in rabbit buccal mucosa has been established. This value can be determined with the following equation from Fick's laws of diffusion:

$$P = [d(Q - M)/dt]/AC_d$$

where $d(Q - M)/dt$ is the change in quantity, Q, of solute minus its metabolites, M, with time, t, A is the exposed area to solute transport, and C_d is the donor concentration of solute. However, this is not the true permeability coefficient of the diffusant in the tissue. In order to calculate this value for TRH, it was necessary to saturate the metabolism capability, M, of the buccal mucosa by, for example, adding an equal and excess amount of the tripeptide to both mucosal and serosal sides of the tissue as was done in the present study.

For each permeability experiment, the total amount of radioactivity transported from the donor to the receiver solution was determined as a percentage of the total donor radioactivity. At the same time, analysis of the receiver and donor solutions for TRH and metabolites was performed with HPLC and radiometric analysis. Metabolism of ^{3}H-TRH was not detected on the mucosal side (i.e., donor chamber) of the tissue, indicating inhibition of TRH deamidase breakdown of ^{3}H-TRH by the excess amount of nonradioactive TRH present. On the serosal side of the tissue, TRH metabolism in the tissue was also drastically inhibited as indicated by the absence of a Pro peak and the largely diminished size of the TRH-OH peak (i.e., 2 to 5% of the total activity present) as represented in Fig. 5.

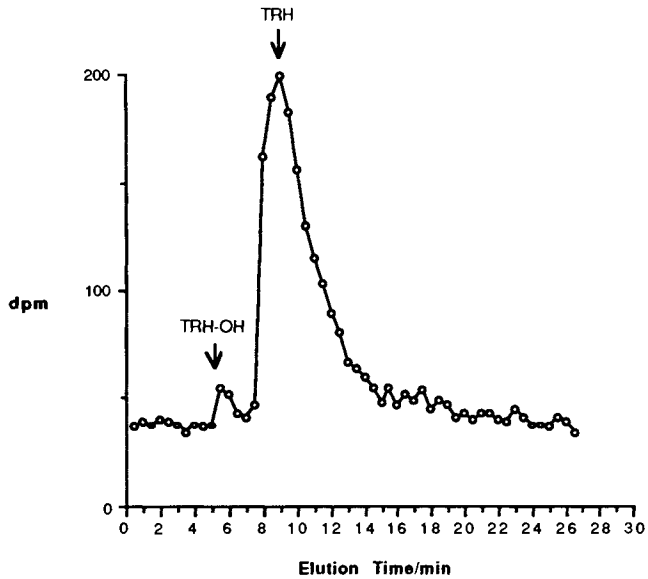

Fig. 5. Radiometric analysis of HPLC eluant from the receiver solution after 120 min at pH 8. Peak areas: 97.6% TRH and 2.4% TRH-OH.

Peak areas were calculated using the trapezoidal rule. Subsequently, the total amount of TRH was determined knowing the total disintegrations per minute of each sample and the percentage of TRH contained therein. The steady-state permeability coefficients of TRH were then calculated with the following equation:

$$P = [(\text{rate of transfer, \% min}^{-1})(1.2\text{ ml})]/[(0.785\text{ cm}^2)(100\%)(60\text{ sec min}^{-1})]$$

where the rate of transfer is the percentage of TRH reaching the receiver solution with time at steady state, 1.2 ml is the volume of the donor chamber, 0.785 cm^2 is the exposed surface area of tissue to transport, 100% is the initial amount in the donor cell, and 60 is the conversion factor for minutes to seconds.

The results of TRH permeability in rabbit buccal mucosa *in vitro* are summarized in Table III. The calculated values are approximately the true permeability coefficients of TRH in the tissue since metabolism was almost completely eliminated. Moreover, the amount of radioactivity being transported with time (i.e., permeability coefficient) was constant for ^{3}H-TRH donor concentrations of (a) 1.7×10^{-5} mM (34) and (b) 1.26×10^{-4} to 4.19×10^{-4} mM (with 83.3 mM cold TRH on both sides of the tissue), implying that the tripeptide traverses rabbit buccal mucosa predominantly by simple diffusion.

The permeability of TRH is independent of bathing buffer pH and, therefore, ionization state of the compound. In general, if the charge density of a compound increases, its permeability in a biological membrane is expected to decrease (35,36). Some possible explanations for the different phenomena observed with TRH permeability include the following: (a) TRH is highly water soluble in both the charged and the uncharged states, and therefore, the degree of solvation may be large for both species—recall that the octanol/water partition coefficient is 0.0376 at pH 7.4 (11), where TRH is greater than 90% uncharged; and (b) TRH moves through the rate-limiting barrier via the same pathway regardless of the charged state of the compound (see below). In effect, the pH partition hypothesis for a diffusing ionizable species in biological membranes may not apply to the diffusion of TRH and, possibly, other largely hydrophilic peptides in buccal mucosa. Recently, Conradi *et al.* (37) have shown that the number of hydrogen bonds plays a greater role than lipophilicity in peptide absorption across Caco-2 cells.

The low buccal penetration rate of TRH may cause

Table III. Mean Permeability Coefficients (P) of TRH in Rabbit Buccal Mucosa *in Vitro* vs pH of the Bathing Buffer at 37°C

Buffer[a]	pH	n[b]	$10^7 \times P$ (cm sec^{-1})
Citric acid	4.0	8	1.3 (±0.3)[c]
HEPES	8.0	8	1.5 (±0.4)

[a] Buffers were used at varied concentrations (i.e., 10–60 mM citric acid and 10–50 mM HEPES) and showed no effect on TRH permeability.

[b] Number of experimental determinations.

[c] Number in parentheses represents the standard error of the mean.

some concern as to the effectiveness of the buccal route to deliver peptides. However, buccal administration of TRH, although only a tripeptide, has been shown to be systemically effective (13,14) without penetration enhancers, indicating that the compound is very potent. From the work of Schurr *et al.* (14), the buccal dose used (i.e., 10 mg) was substantially greater than that used i.v. (i.e., 0.4 mg) due to the obvious high resistance of the epithelium and possibly metabolism (depending on the activity of TRH-OH). Moreover, the buccal route showed a slower onset of thyrotropin and prolactin levels and less rapid elimination kinetics (i.e., depot effect) and was without side effects (i.e., limited absorption) compared to the i.v. route. Plasma levels of thyrotropin and prolactin from nasal administration (i.e., 1 mg) of TRH were closer to those i.v., while GI administration (i.e., 40 mg) of the tripeptide was more similar to buccal delivery.

TRH Pathway and Rate-Limiting Barrier Studies

Microautoradiography. Representative micrographs of the overall results are shown in Figs. 6 through 8. Control micrographs showed no grains (Fig. 6), and moreover, there was no apparent negative chemography (photo not shown). When TRH is applied to the mucosal surface only, the grain density is sparse and uniform throughout the tissue section (Fig. 7). However, when the tripeptide is placed on the serosal surface only (Fig. 8), the grain density is much greater in the lower, more viable epithelial cell layers until it reaches within approximately 50 μm of the surface, where the grain density is similar to that seen in Fig. 7. This indicates that TRH and its metabolites (i.e., tritiated TRH-OH and Pro) move more easily through the lower epithelial region relative to the upper cell layers. Consequently, the rate-limiting barrier for TRH can be defined as being in the upper 50 μm of rabbit buccal epithelium, which, incidentally, has been shown to be in the same area for other penetrants (16,38–41).

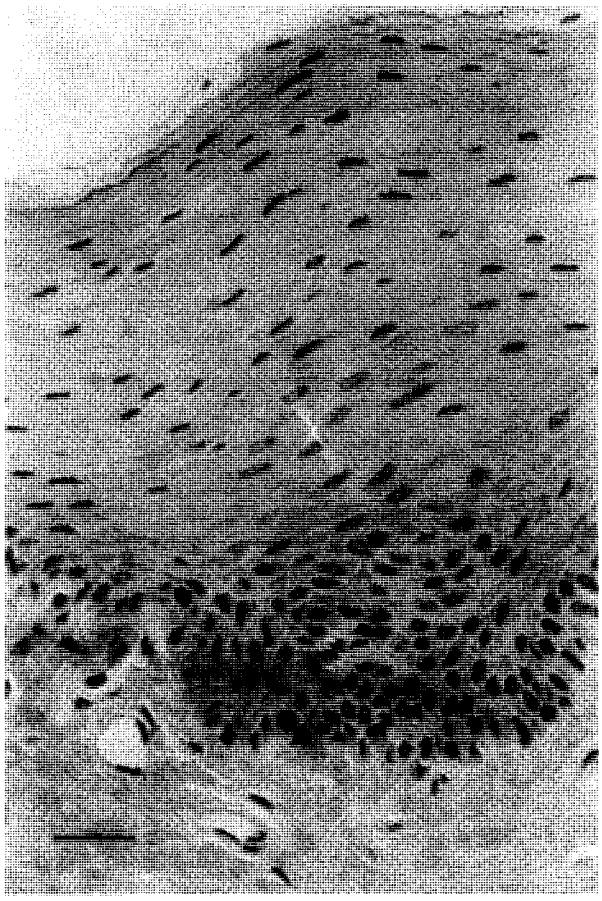

Fig. 6. Control rabbit buccal mucosa (3-μm section) without radiolabeled TRH showing no grain formation (8-week exposure). Bar represents 20 μm.

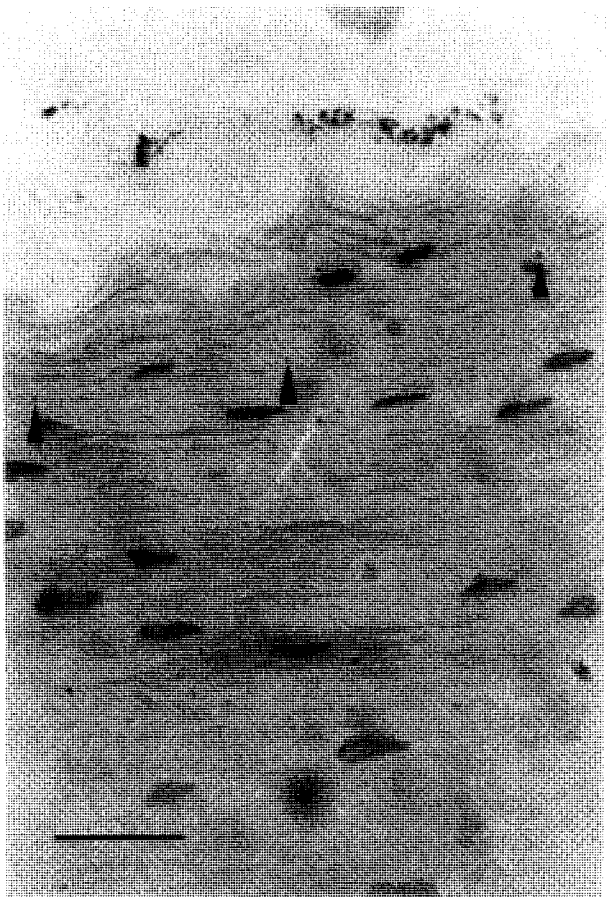

Fig. 7. ^{3}H-TRH applied to the mucosal surface of rabbit buccal mucosa only (2-μm section) showing a sparse and uniform grain density throughout the epithelial cell layers (6-week exposure). Grains appear to be located predominantly in the paracellular space in the upper 50 μm or so of the epithelium (arrowheads). Lighter grains at the surface of the epithelium are TRH, however, darker spots are from the toluidine blue stain. Bar represents 20 μm.

Numerical analysis of grain distributions in 20 autoradiographs (12-week exposure) is summarized in Table IV. It appears that the paracellular pathway is the most important route for TRH movement, at least through the upper 50 μm of the epithelium, where grains are located primarily in the intercellular space. However, since the intercellular space is about 0.2 μm (15) and, furthermore, since there is about a 0.5-μm uncertainty associated with the position of the grains and the location of TRH (42), the position of grains in the

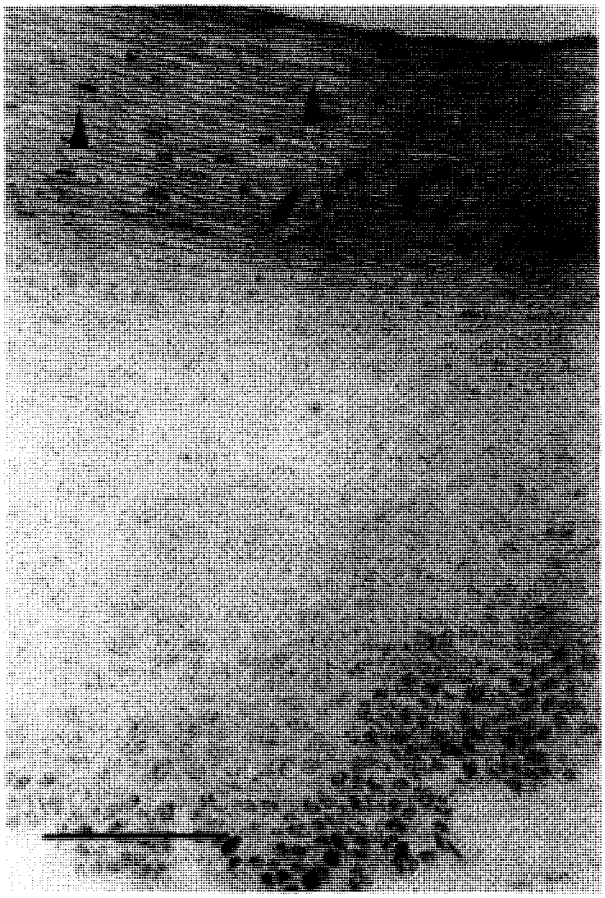

Fig. 8. ^{3}H-TRH applied to the serosal surface of rabbit buccal mucosa only (2-μm section) showing a large concentration of grains in the lower epithelial layers (8-week exposure). However, the grain density suddenly changes at approximately 50 μm from the surface (arrowheads). Comparing this result with Fig. 7 indicates that the rate-limiting barrier is in the upper epithelial cell layers. Furthermore, grains are located predominantly in the paracellular space in the rate-limiting barrier. Bar represents 50 μm.

intercellular region does not exclude the possibility of TRH internalization close to the membrane. For this reason, osmolarity experiments were performed which strengthen the argument for a paracellular route of transport (see below). On the other hand, in the more viable cell layers below this region, grains were equally distributed both intercellularly and intracellularly. Consequently, it is not clear exactly where TRH may be in the lower cell layers since the tripeptide is metabolized.

Table IV. Numerical Analysis of TRH Grain Distribution in Rabbit Buccal Mucosa *in Vitro*

Upper 50 μm (rate-limiting step)	
Grains located in the intercellular space	81% (±3%)[a]
Grains located intracellularly	4% (±1%)
Grains located on the border line	15% (±3%)
Below the rate-limiting step	
Grains located equally between both intercellular and intracellular regions	

[a] Number in parentheses represents the standard error of the mean.

The differences in grain distribution in these two regions may be attributed to differences in physical characteristics of cells in the rate-limiting barrier and the more viable cell layers (43). For example, the plasma membrane is greatly thickened in the upper spinous cells, i.e., in the presence of a cross-linked chemical-resistant cell envelope, which may not allow a solute easy access into the cell. Moreover, phospholipase activity appears to be absent in this region (40), suggesting that the chemical state of phospholipids has been modified, possibly by enzymes contained in membrane coating granules (see below). Another difference between the upper and the lower cells is that as cells migrate toward the surface, they experience a loss of cellular organelles (15), in particular, mitochondria, ribosomes, golgi complexes, and endoplasmic reticulum, which may be an indication of the cells' ability to perform activities such as active transport or endocytic processes.

The barrier region is also coincident with the extruded contents of membrane coating granules (MCGs), which may play a major role in the formation of the permeability barrier (44–46). Note in Fig. 8 that the staining of protein–carbohydrate complexes increases in intensity toward the surface (i.e., increase in gray color in the intercellular spaces), indicating an increase in the presence of this intercellular substance as cells migrate toward the surface. However, the abrupt reduction in grain density at the border of the rate-limiting barrier does not correlate with the increase in intercellular material. This very drastic change could then be associated with, for example, enzymes from MCGs (47,48) being released into the intercellular space, which may rapidly change the physicochemical properties of the materials present, in particular, the protein–carbohydrate substances, as well as cell membrane components. Evidence for this comes from studies showing changes in lectin binding between the upper and the lower epithelial regions (49).

Osmolarity Experiments. The steady-state permeability of TRH (calculated as described above) under both hypotonic and hypertonic conditions relative to its permeability in isotonic conditions was plotted against the osmolarity of the bathing buffer, as depicted in Fig. 9. The permeability of TRH, in both its charged (pH 4) and its uncharged (pH 8) forms, shows a similar trend with both hypotonic or hypertonic tissue challenges. The effect of osmolarity on the permeability of a solute in a mucosal membrane should indicate the transport pathway. The regulation of animal cell volume in response to an osmotic challenge is accomplished initially by a rapid water flux across the plasma membrane, followed by a slower cell volume recovery via ion redistribution through channels or transporters (50–55). When the bathing solution is isotonic, there is no net flux of water. However, if the bathing medium is hypotonic or hypertonic, water will flow into or out of the cell, respectively, until osmotic pressure is equalized outside and inside the cell. Cell volume can subsequently return toward normal levels via plasma membrane transporters such as the Na^+/K^+ ATPase pump, N^+/H^+ exchanger, $K^+/Na^+/Cl^-$ cotransporter, and Cl^-/HCO_3^- exchanger as well as ion channels.

If ions in the bathing solution are removed and the osmotic insult is caused by a nontransportable solute, such as

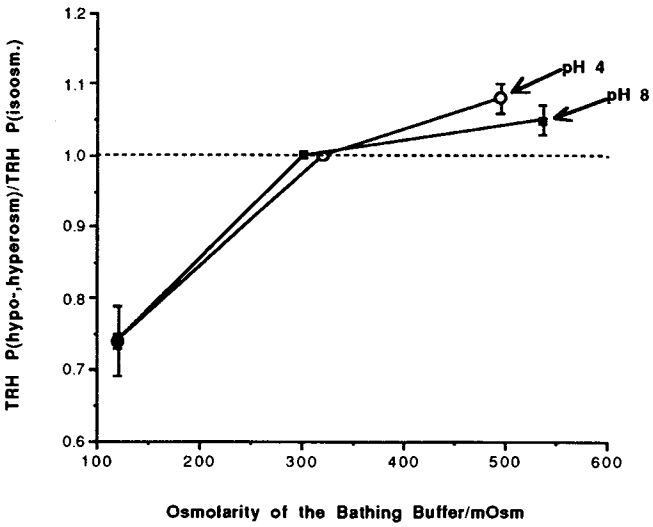

Fig. 9. The effect of osmolarity on the permeability of TRH in rabbit buccal mucosa *in vitro*. Summary of at least four experiments for each point. Hypotonic and hypertonic TRH permeability values relative to isotonic TRH permeability values are plotted against the osmolarity of the bathing buffer. Error bars represent the standard error of the mean. The dashed line is for reference only.

mannitol, the cells should not be able to regulate their plasma volume back toward normal levels. A swollen or shrunken cell state should persist with a respective hypotonic or hypertonic challenge. In these experiments, the permeability coefficient was constant at steady state for the duration of the experiment, suggesting that this was the case. Consequently, if a solute traversing an epithelium by simple diffusion utilizes predominantly the paracellular pathway, it should experience a significant decline or enhancement in permeability if the bathing medium is hypotonic or hypertonic, respectively. In the former case, the cells are presumably more closely packed together, resulting in a smaller intercellular opening and, therefore, a decrease in solute flux, while in the latter case, the intercellular space is wider and solute flux should be enhanced. Therefore, the paracellular pathway appears to be the major conducting route for TRH, at least in the rate-limiting barrier, irrespective of the ionization state of the peptide which is in agreement with autoradiography results.

The nonlinearity in Fig. 9 may be due to differences in the ability of the cells to expand and contract (cells may readily push up closer to each other, whereas the adhesive nature of the intercellular material, and possibly desmosomes, may hinder cells from shrinking apart).

CONCLUSIONS

TRH moves through the buccal tissue via simple diffusion experiencing both a highly resistant barrier in the upper 50 μm of the epithelium and biphasic enzymatic degradation. The steady-state TRH permeability of 10^{-7} cm/sec is independent of the bathing buffer pH and, therefore, the ionization state of the tripeptide, possibly because of the similar hydrophilicity properties of TRH in both the charged and the uncharged states and the physicochemical properties of the epithelium allowing only paracellular diffusion in the rate-limiting barrier. The low penetrability of TRH in buccal mucosa is therapeutically effective if a sufficiently high concentration is used. However, penetration enhancers and enzyme inhibitors may be necessary for successful therapy of larger peptides such as insulin (9,56). Penetration enhancement should modify the paracellular space of the rate-limiting barrier to achieve the most efficient delivery of TRH through buccal mucosa without additional damage to cell membranes.

REFERENCES

1. J. M. Samanen. Polypeptides as drugs. *Polym. Mater. Sci. Eng.* 51:193–197 (1984).
2. B. L. Ferraiolo and L. Z. Benet. Peptides and proteins as drugs. *Pharm. Res.* 2:151–156 (1985).
3. V. H. L. Lee. Peptide and protein drug delivery: Opportunities and challenges. *Pharm. Int.* 7:208–212 (1986).
4. O. Siddiqui and Y. W. Chien. Nonparenteral administration of peptide and protein drugs. *CRC Crit. Rev. Ther. Drug Carrier Syst.* 3:195–208 (1987).
5. H. M. Patel (ed.). Peptide drug delivery. *Biochem. Soc. Trans.* 17:931–949 (1988).
6. V. H. L. Lee (ed.). *Peptide and Protein Drug Delivery,* Marcel Dekker, New York, 1990.
7. V. H. L. Lee. Trends in peptide and protein drug delivery. *Biopharm* 4:22–25 (1991).
8. W. R. Galey, H. K. Lonsdale, and S. Nacht. The in vitro permeability of skin and buccal mucosa to selected drugs and tritiated water. *J. Invest. Dermatol.* 67:713–717 (1976).
9. J. Zhang, C. D. Ebert, H. Gijsman, S. McJames, and T. H. Stanley. Trans-buccal mucosal delivery of insulin: An in vivo dog model. *Pharm. Res.* 7:S-116 (1990).
10. R. R. Burnette and D. Marrero. Comparison between the iontophoretic and passive transport of thyrotropin releasing hormone across excised nude mouse skin. *J. Pharm. Sci.* 75:738–743 (1986).
11. V. H. L. Lee. Enzymatic barriers to peptide and protein absorption. *CRC Crit. Rev. Ther. Drug Carrier Syst.* 5:69–97 (1988).
12. A. G. Gilman, L. S. Goodman, T. W. Rall, and F. Murad (eds.). *Goodman and Gilman's The Pharmacological Basis of Therapeutics,* Macmillan, New York, 1985.
13. R. Anders, H. P. Merkle, W. Schurr, and R. Ziegler. Buccal absorption of protirelin: An effective way to stimulate thyrotropin and prolactin. *J. Pharm. Sci.* 72:1481–1483 (1983).
14. W. Schurr, B. Knoll, R. Ziegler, R. Anders, and H. P. Merkle. Comparative study of intravenous, nasal, oral and buccal TRH administration among healthy subjects. *J. Endocrinol. Invest.* 8:41–44 (1985).
15. S. Y. Chen. *Comparison of the Fine Structure of the Mucosa of Cheek and Hard Palate in the Rabbit,* M.S. thesis, University of Illinois, Chicago, 1970.
16. C. A. Squier. The permeability of keratinized and nonkeratinized oral epithelium to horseradish peroxidase. *J. Ultrastruct. Res.* 43:160–177 (1973).
17. D. Adams. The mucus barrier and absorption through the oral mucosa. *J. Dent. Res.* 54:B19–B26 (1975).
18. S. Y. Chen and C. A. Squier. The ultrastructure of the oral epithelium. In J. Meyer, C. A. Squier, and S. J. Gerson (eds.), *The Structure and Function of Oral Mucosa,* Pergamon Press, New York, 1984, pp. 7–30.
19. M. E. Dowty. *Transport of Thyrotropin Releasing Hormone in Rabbit Buccal Mucosa in Vitro,* Ph.D. thesis, University of Wisconsin, Madison, 1991.
20. M. A. Longer. *Characterization of Buccal Epithelia Relevant to Peptide Drug Delivery,* Ph.D. thesis, University of Wisconsin, Madison, 1988.
21. C. A. Lesch, C. A. Squier, A. Cruchley, D. M. Williams, and P. Speight. The permeability of human oral mucosa and skin to water. *J. Dent. Res.* 68:1345–1349 (1989).

22. I. A. Siegel, K. T. Izutsu, and E. Watson. Mechanisms of nonelectrolyte penetration across dog and rabbit oral mucosa in vitro. *Arch Oral Biol.* **26**:357–361 (1981).
23. R. D. Schoenwald and H. S. Huang. Corneal penetration behavior of β-blocking agents I: Physiochemical factors. *J. Pharm. Sci.* **72**:1266–1272 (1983).
24. M. M. Veillard, M. A. Longer, T. W. Martens, and J. R. Robinson. Preliminary studies of oral mucosal delivery of peptide drugs. *J. Control. Release* **6**:123–131 (1987).
25. H. F. Edelhauser, J. R. Hoffert, and P. O. Fromm. In vitro ion and water movement in corneas of rainbow trout. *Invest. Ophthalmol.* 4:290–296 (1965).
26. G. M. Grass and S. A. Sweetana. In vitro measurement of gastrointestinal tissue permeability using a new diffusion cell. *Pharm. Res.* 5:372–376 (1988).
27. J. Blanchard. Evaluation of the relative efficacy of various techniques for deproteinizing plasma samples prior to HPLC analysis. *J. Chromatogr.* **226**:455–460 (1981).
28. I. G. Tucker, M. E. Dowty, M. Veillard, M. A. Longer, and J. R. Robinson. Reverse phase HPLC analysis of oligoglycines (one to six amino acid residues). *Pharm. Res.* **6**:100–102 (1989).
29. R. E. Stratford and V. H. L. Lee. Aminopeptidase activity in homogenates of various absorptive mucosae in the albino rabbit: Implications in peptide delivery. *Int. J. Pharm.* **30**:73–82 (1986).
30. K. W. Garren and A. J. Repta. Buccal drug absorption I: Comparative levels of esterase and peptidase activities in rat and hamster buccal and intestinal homogenates. *Int. J. Pharm.* **48**:189–194 (1988).
31. V. H. L. Lee, R. D. Traver, and M. E. Taub. Enzymatic barriers to peptide and protein drug delivery. In V. H. L. Lee (ed.), *Peptide and Protein Drug Delivery,* Marcel Dekker, New York, 1991, pp. 303–358.
32. D. B. Guzek, A. H. Kennedy, S. C. McNeill, E. Wakshull, and R. O. Potts. Transdermal drug transport and metabolism I. Comparison of in vitro and in vivo results. *Pharm. Res.* **6**:33–39 (1989).
33. R. O. Potts, S. C. McNeill, C. R. Desbonnet, and E. Wakshull. Transdermal drug transport and metabolism II. The role of competing kinetic events. *Pharm. Res.* **6**:119–124 (1989).
34. M. E. Dowty. *Permeability of Thyrotropin Releasing Hormone in Rabbit Buccal Mucosa in Vitro,* M.S. thesis, University of Wisconsin, Madison, 1988.
35. M. H. Bickel and H. J. Weder. Buccal absorption and other properties of pharmacokinetic importance of imipramine and its metabolites. *J. Pharm. Pharmacol.* **21**:169–175 (1969).
36. S. Bergman, D. Kane, I. A. Siegel, and S. Ciancio. In vitro and in situ transfer of local anaesthetics across the oral mucosa. *Arch. Oral Biol.* 14:35–43 (1969).
37. R. A. Conradi, A. R. Hilgers, N. F. H. Ho, and P. S. Burton. The influence of peptide structure on transport across Caco-2 cells. *Pharm. Res.* **8**:1453–1460 (1991).
38. C. A. Squier and L. Rooney. The permeability of keratinized and nonkeratinized oral epithelium to lanthanum in vivo. *J. Ultrastruct. Res.* **54**:286–295 (1976).
39. M. W. Hill, C. A. Squier, and J. E. Linder. A histological method for the visualization of the intercellular permeability barrier in mammalian stratified squamous epithelia. *Histochem. J.* **14**:641–648 (1982).
40. C. A. Squier. Effect of enzyme digestion on the permeability barrier in keratinizing and nonkeratinizing epithelia. *Br. J. Dermatol.* 3:253–264 (1984).
41. C. A. Squier and B. K. Hall. In vitro permeability of porcine oral mucosa after epithelial separation, stripping and hydration. *Arch. Oral Biol.* **30**:485–491 (1985).
42. A. W. Rogers. *Techniques of Autoradiography,* 3rd ed., Elsevier Press, New York, 1979.
43. J. Meyer, C. A. Squier, and S. J. Gerson (eds.). *The Structure and Function of Oral Mucosa,* Pergamon Press, New York, 1984.
44. P. W. Wertz and C. A. Squier. Cellular and molecular basis of barrier function in oral epithelium. *CRC Crit. Rev. Ther. Drug Carrier Syst.* 8:237–269 (1991).
45. A. F. Hayward and M. Hackemann. Electron microscopy of membrane-coating granules and a cell surface coat in keratinized and nonkeratinized human oral epithelium. *J. Ultrastruct. Res.* 43:205–219 (1973).
46. C. A. Squier. Membrane coating granules in nonkeratinizing oral epithelium. *J. Ultrastruct. Res.* **60**:212–220 (1977).
47. S. Silverman and G. Kearns. Ultrastructural localization of acid phosphatase in human buccal mucosa. *Arch. Oral Biol.* **15**:169–177 (1970).
48. A. F. Hayward. Membrane-coating granules. *Int. Rev. Cytol.* 59:97–127 (1979).
49. E. Dabelsteen. Receptors on the keratinocyte surface. In J. Meyer, C. A. Squier, and S. J. Gerson (eds.), *The Structure and Function of Oral Mucosa,* Pergamon Press, New York, 1984, pp. 83–93.
50. S. Grinstein, S. Cohen, J. D. Goetz, and A. Rothstein. Na/H exchange in volume regulation and cytoplasmic pH homeostasis in lymphocytes. *Fed. Proc.* **44**:2508–2512 (1985).
51. E. K. Hoffman. Role of separate K and Cl channels and of Na/Cl cotransport in volume regulation in Ehrlich cells. *Fed. Proc.* **44**:2513–2519 (1985).
52. C. W. Davis and A. L. Finn. Cell volume regulation in frog urinary bladder. *Fed. Proc.* 44:2520–2525 (1985).
53. K. R. Spring. Determinants of epithelial cell volume. *Fed. Proc.* **44**:2526–2529 (1985).
54. B. Alberts, D. Bray, J. Lewis, M. Raff, K. Roberts, and J. D. Watson. *Molecular Biology of the Cell,* 2nd ed., Garland, New York, 1989.
55. J. Darnell, H. Lodish, and D. Baltimore. *Molecular Cell Biology,* 2nd ed., Scientific American Books, New York, 1990.
56. M. Ishida, Y. Machida, N. Nambu, and T. Nagai. New mucosal dosage form of insulin. *Chem. Pharm. Bull.* **29**:810–816 (1981).